Supplemental Information

Peripheral Protein Unfolding Drives Membrane Bending

Hew Ming Helen Siaw, Gokul Raghunath, R. Brian Dyer*

Department of Chemistry, Emory University, 1515 Dickey Drive, Atlanta, Georgia 30322, United States

*Corresponding author (briandyer@emory.edu)

CONTENTS

SUPPLEMENTARY MATERIALS AND METHODS:

Materials

Coomassie Brilliant Blue R-250 Dye, 5,5-dithio-bis-(2-nitrobenzoic acid) (DTNB) were purchased from ThermoFisher SCIENTIFIC (Waltham, MA). Uranyl acetate, methanol, acetic acid (glacial, ≥99.85%), 8-Anilino-1-naphthalenesulfonic acid (ANS) were obtained from SIGMA-ALDRICH® (St. Louis, MO). Blue Prestained Protein Standard, Broad Range was purchased from New England Biolabs Inc. (Ipswich, MA). Native sample buffer for protein gels and Mini PROTEAN®TGX™ Precast Gels were obtained from Bio-Rad (Hercules, CA). Carbon 200 mesh, Copper grids were obtained from (Electron Microscopy Sciences, Hatfield, PA).

Human Serum Albumin Unfolding Characterization

Tryptophan Fluorescence Emission

Time dependent tryptophan fluorescence measurements were performed by incubating 20 μM human serum albumin with 200 mM DTT for 10 mins, 30 mins, 1 hour, and 2 hours.

ANS Fluorescence Emission

20 μM human serum albumin (final concentration) was incubated with various concentrations of DTT (10 mM, 20 mM, 30 mM, 40 mM, 50 mM, 60 mM, 70 mM, 80 mM, 90 mM, 100 mM) and 50 μM ANS (final concentration) for 2 hours. Fluorescence spectra were collected by excitation at 372 nm with an integration time of 1 s over total range of 285-550 nm.

Effect of HSA unfolding on liposomes

Dynamic light scattering measurement (DLS)

1 μM His-tagged human serum albumin was added to 2 mM PSL or NPSL with 10 mol% or 20 mol% or 30 mol% Ni-NTA-DGS and incubated with or without 10 mM DTT for 2 hours. 80 μL of each sample was transferred to a 1 cm quartz cuvette and data were collected with a NanoPlus-Zeta/Nano Particle Analyzer (Particulate Systems, Norcross, GA). 3x30 measurement runs were performed, with standard setting (Refractive index = 1.331, viscosity= 0.88, temperature = 25 ^{o}C)

Autocorrelation functions of each data set were fitted to single exponential equation to obtain decay time (τ).

$$Ae^{\frac{-t}{\tau}}$$

, where t is overall time course of decay in μs, and τ is the decay time.

Electron microscopy imaging

Carbon 200 mesh, copper grids were glow discharged at 10 mA for 45 s with a sputter coater prior to application of any materials. PSL and NPSL incubated with His-tagged HSA and His-tagged HSA with DTT were diluted with buffer to 0.1 mM prior applying to grids for 1 min. Excess samples were removed from grids by buffer rinse and filter paper blotting. As a control, PSL, NPSL with or without DTT were also applied to grids for 1 min. Afterwards, grids were stained with 1% uranyl acetate for 1 min, then air dried at room temperature. Images were taken with a Hitachi HT-7700 transmission electron microscope at 80 kV accelerating voltage.

Protein Labelling

Ellman's Test

To quantify the number of free sulfhydryl group on His-tagged HSA for the conjugation to Alexa488 fluorescence dye with a maleimide linkage, 4mg of DTNB was dissolved in sample buffer (0.1 M Sodium phosphate, 1 mM EDTA, pH 8.0). A set of sulfhydryl standards (cysteine hydrochloride monohydrate) with concentrations of 1.5 mM, 1.25 mM, 1.0 mM, 0.75 mM, 0.5 mM, and 0.25 mM were prepared with sample buffer. A 0.5 mM HSA solution was pre-incubated with 1 mM TCEP for 15 mins. Then 250μL sample/standard, 2.5 mL sample buffer, 50 μL DTNB reagent were mixed in test tubes, incubated for 15 mins and the absorbance was measured at $\lambda_{412\,nm}$ with a Lambda35 UV/Vis spectrophotometer (Perkin Elmer, Waltham, MA). The concentration of sulfhydryl group was determined using a standard curve derived from the CysHCl standards, and with the molar extinction coefficient of DTNB at $\lambda_{412\,nm}$ (14,150 $M^{-1}cm^{-}$)[6]. We determined that this human serum albumin preparation (Sigma; lot number SLBL5290V) contained 0.51 mol –SH/mol protein.

His-tagged HSA labelling

His-tagged HSA was dissolved in 100 mM PBS (BupH Phosphate Buffered Saline Packs, ThermoFisher Scientific, Waltham, MA). The labelling reactions were performed with the thiol-reaction using maleimide functionalized dye (Alexa488 C5 Maleimide). Protein was first incubated with 10-fold molar excess of TCEP at room temperature for 1 hour, then incubated with 10 fold molar excess dye at 4 ^{o}C, stirred overnight in the dark. Upon completion of the reaction, excess glutathione was added to the solution, then stirred for 30 mins at room temperature. Excess dye molecules were removed using a ZebraSpin Desalting Column with a 7K MW cutoff (ThermoFisher Scientific, Waltham, MA).

Native Page to compare molecular weight of HSA vs. HSA reduced by DTT

HSA was dissolved in buffer to a concentration of 1.5 mg/mL. To prepare the unfolded sample, the 1.5 mg/mL solution of HSA was incubated with 200 mM DTT for 2 hours at room temperature. Samples were diluted 1:3 in native page buffer and run on a precast gel for 2 hours at 100 V, 160 mA on ice with Tris-Glycine native running buffer. Afterwards, the gel was stained with Coomassie Blue staining solution (0.1% Coomassie Blue R230, 50% MeOH, 7% acetic acid) for 15 mins, then destained with destaining solution (5% MeOH, 7% acetic acid) overnight at room temperature.

Equilibrium ATR-FTIR of phase separated supported lipid bilayer (containing 30 mol% of Ni-NTA-DGS) with 100mM or 1M $NiCl_2$

Cleaning of germanium crystal and preparation of phase separated supported lipid bilayer were performed according to protocol in the method section. A buffer spectrum was collected before introducing the lipids and was used a background spectrum for subsequent measurement. Supported lipid bilayer was incubated on the crystal surface for 30 minutes. Buffer was flushed through the cell to rinse away any excess vesicles. The supported lipid bilayer spectrum was taken. Afterwards, $NiCl_2$ (100mM or 1M as final concentration) was added and incubated with the bilayer for 15 minutes, then obtained a spectrum. Each spectrum was obtained with an average of 256 scans at 2 cm^{-1} resolution.

SUPPLEMENTAL FIGURES:

1. Characterization of the DTT induced unfolding of HSA. In Figure S1, we showed that there was a change in the hydrodynamic radius of HSA once incubated with DTT for 2 hours. From the autocorrelation function of unfolded HSA, it is shown that particles diffuse much slower than folded HSA.

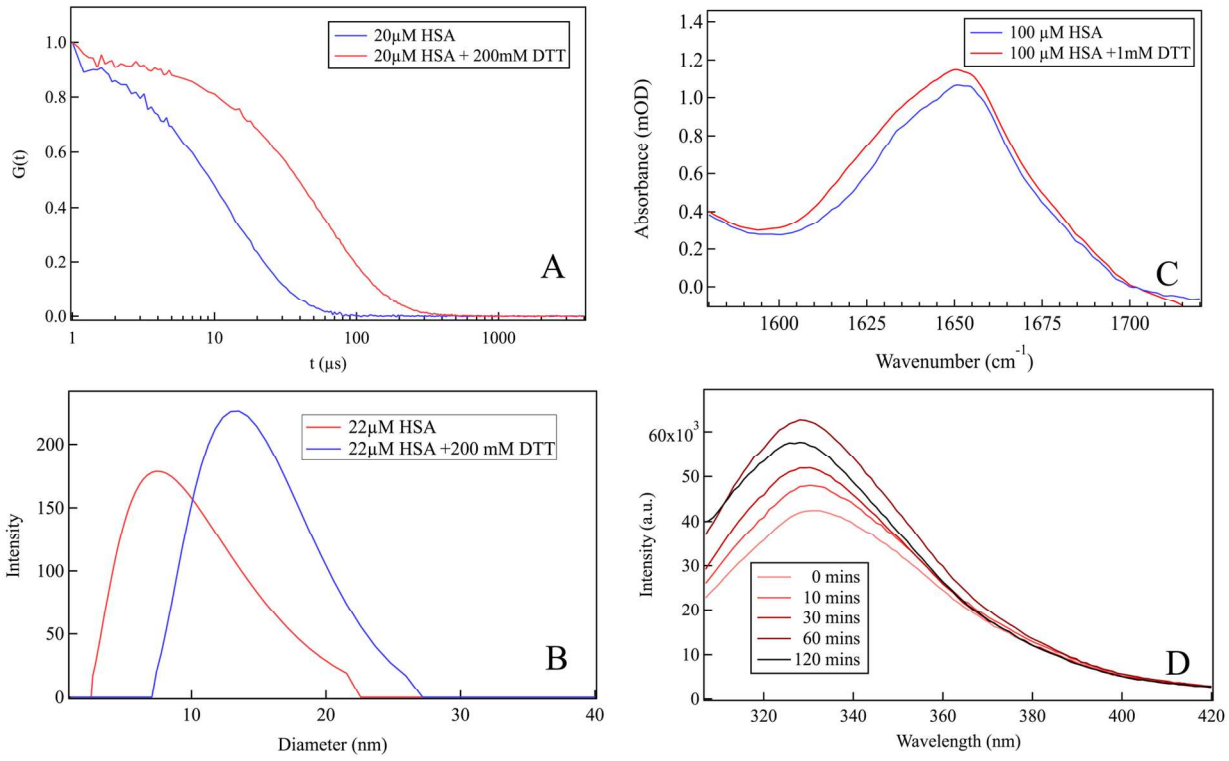

Figure S1. Characterization of HSA unfolding under reducing conditions. A. Dynamic light scattering autocorrelation function of unfolded HSA shows slower decay than folded HSA. B. Calculated DLS intensity profile of unfolded HSA versus folded HSA, showcasing the difference in hydrodynamic radii. C. Equilibrium ATR-FTIR absorbance spectrum in the Amide I' region. Spectra are normalized at 1550 cm^{-1} for comparison. D. Time dependent tryptophan fluorescence measurement of HSA in the presence of DTT. The graph shows blue shift in emission maxima in time dependent fashion.

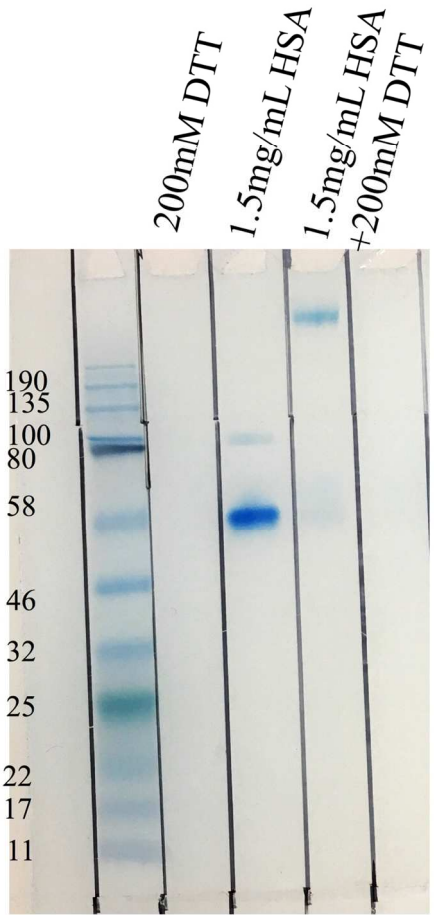

Figure S2. Native page of HSA and HSA unfolded with DTT. The lane containing HSA shows a band at 58 kD as expected for the native protein. In contrast, the lane containing unfolded HSA shows a band that is out of range of the protein standards, clearly indicating unfolding of the protein.

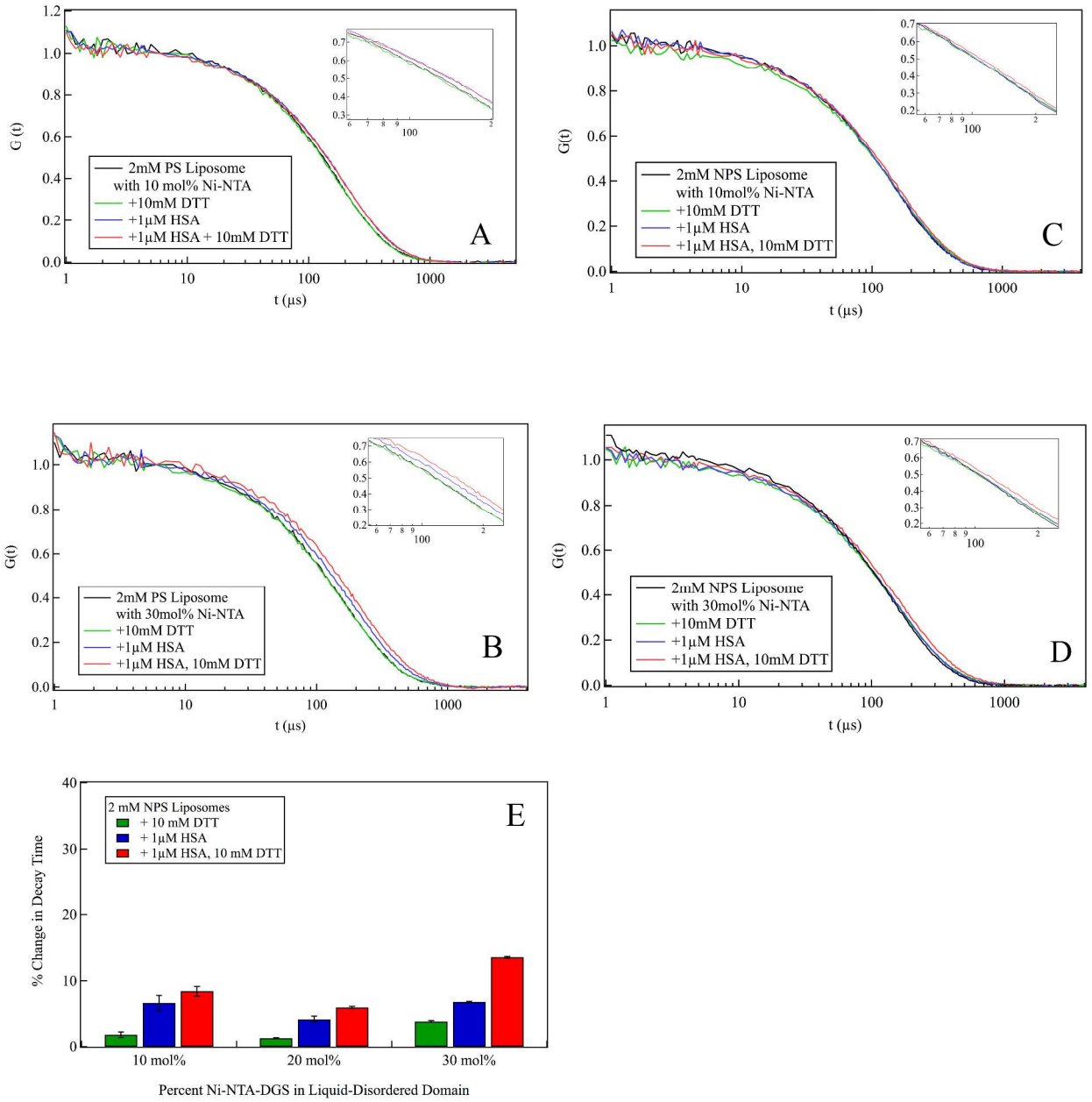

Figure S3. Normalized autocorrelation functions and hydrodynamic radii of PSL and NPSL containing 10 mol%, 20 mol%, and 30 mol% Ni-NTA-DGS in the presence of folded HSA and unfolded HSA. A. PSL with 10 mol% Ni-NTA shows overlapping traces for folded and unfolded HSA samples. B. PSL with 30 mol% Ni-NTA shows a slower decay in unfolded HSA than folded HSA. C. NPSL with 10 mol% Ni-NTA shows a slight difference in decay between folded and unfolded HSA D. NPSL with 30 mol% Ni-NTA shows a slower decay in unfolded HSA than folded HSA. E. Percent change in decay time of NPSL doped with 10 mol% , 20 mol% , and 30 mol% Ni-NTA-DGS in the presence of folded and unfolded HSA. Decay times were obtained by fitting autocorrelation traces to single exponential.

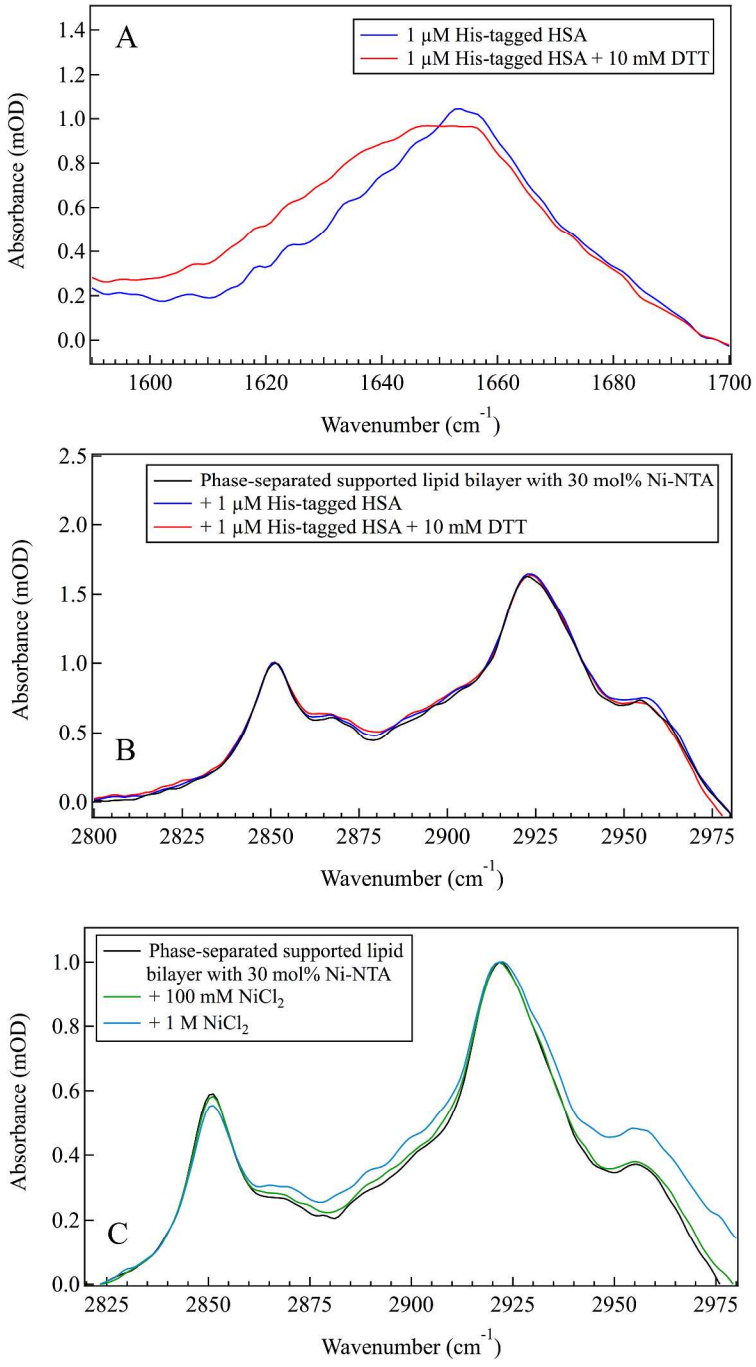

Figure S4. Equilibrium ATR-FTIR performed on supported lipid bilayer containing 30 mol% Ni-NTA-DGS in liquid-disordered phase. A. Equilibrium ATR-FTIR absorbance spectrum in the Amide I' region of folded (blue trace) and unfolded HSA (red trace). B. Absorbance spectrum of C-H stretching region of lipid with bound, folded HSA (blue trace) and HSA unfolded with DTT (red trace). C. Absorbance spectrum of C-H stretching region of lipid with 100 mM $NiCl_2$ (green trace) and 1 M $NiCl_2$ (blue trace).

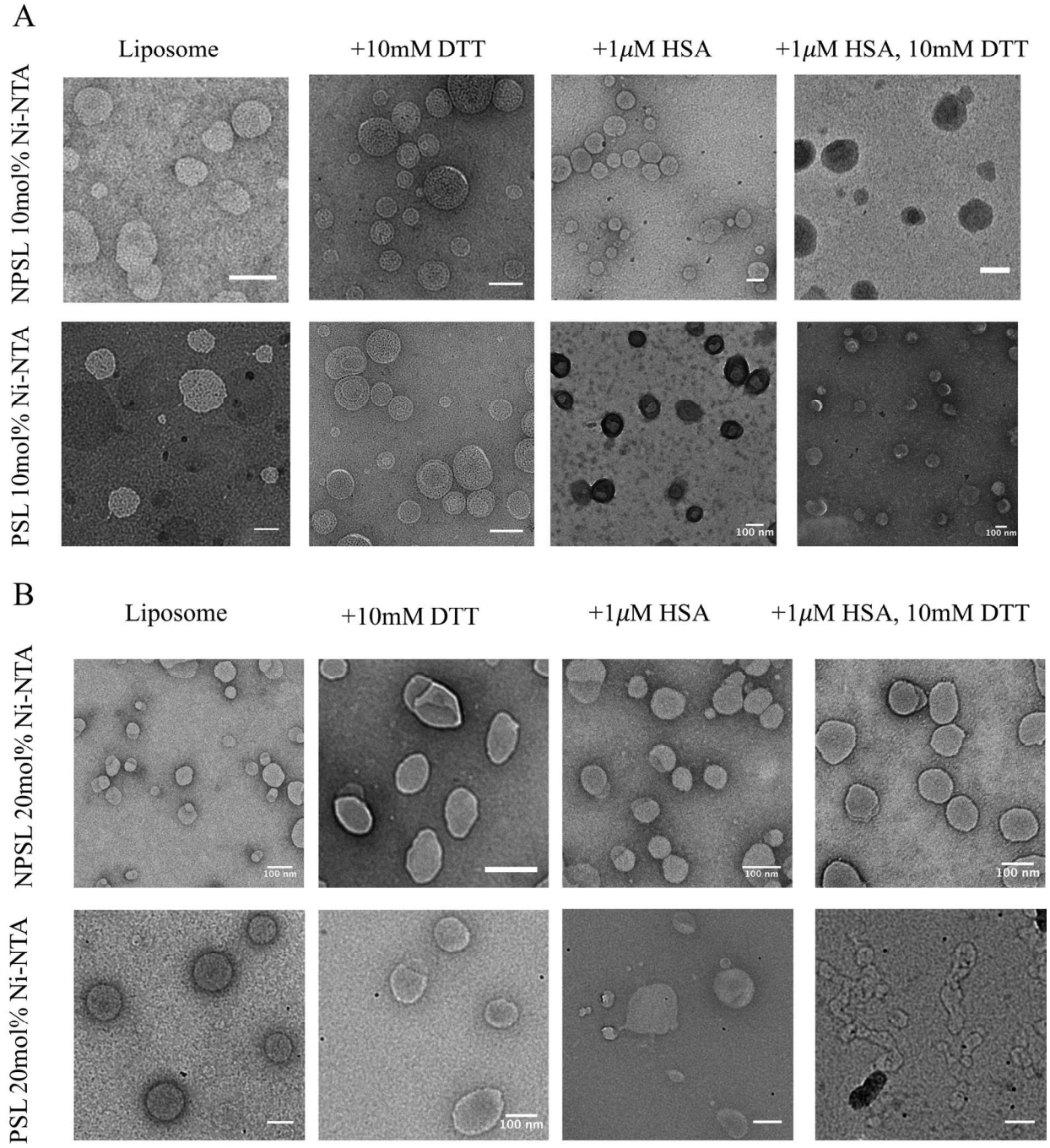
A
Liposome
+10mM DTT
+1μM HSA
+1μM HSA, 10mM DTT
NPSL 10mol% Ni-NTA
PSL 10mol% Ni-NTA
100 nm
B
Liposome
+10mM DTT
+1μM HSA
+1μM HSA, 10mM DTT
NPSL 20mol% Ni-NTA
PSL 20mol% Ni-NTA
100 nm

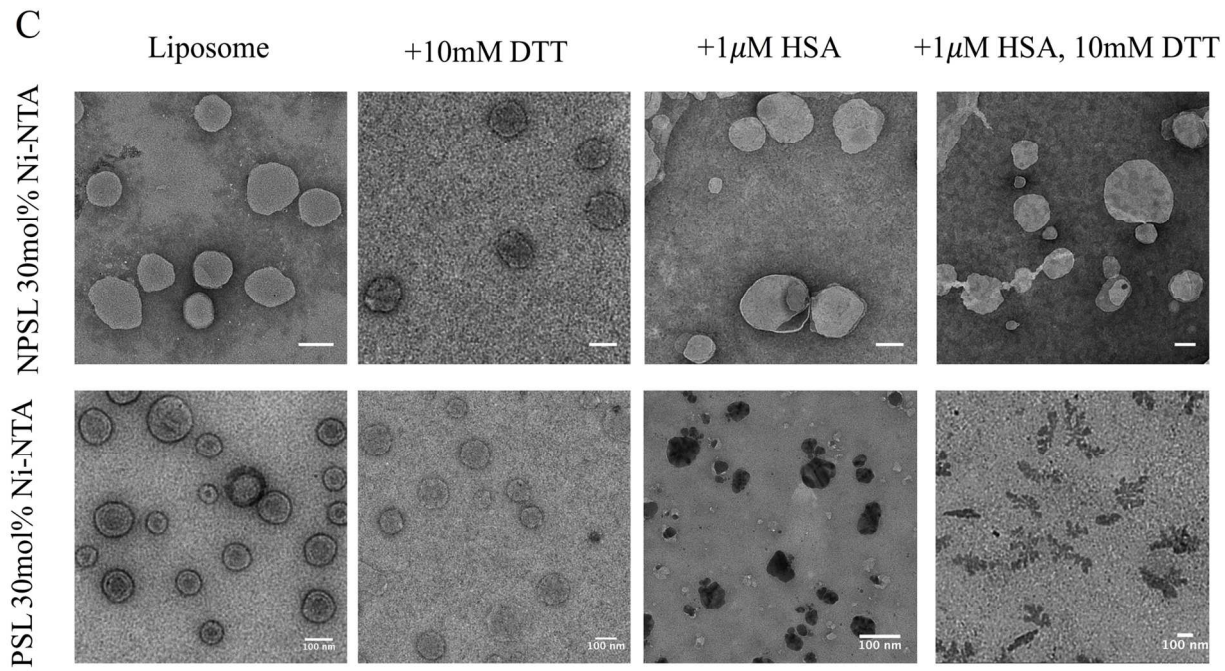

Figure S5. TEM images of PSL and NPSL with 10 mol%, 20 mol%, and 30 mol% of Ni-NTA-DGS in the presence of DTT, folded HSA, and unfolded HSA. A. TEM images of NPSL and PSL with 10 mol% Ni-NTA DGS show no difference in morphology. B. TEM images of NPSL and PSL doped with 20 mol% Ni-NTA C. TEM images of NPSL and PSL doped with 30 mol% Ni-NTA.

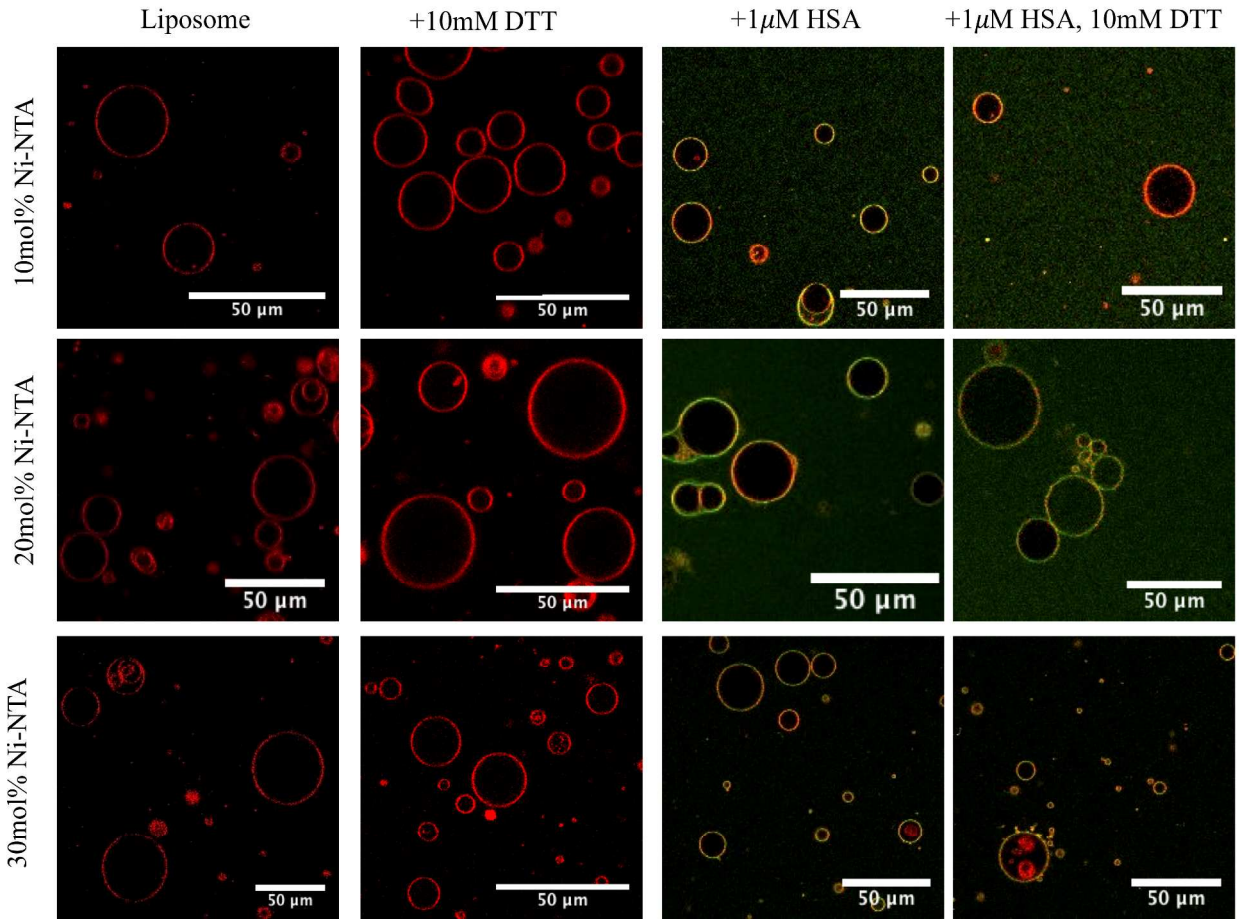

Figure S6. Confocal fluorescence images of NPS GUV doped with 10 mol%, 20 mol%, and 30 mol% Ni-NTA-DGS in the presence of DTT, folded HSA, and unfolded HSA. The red channel monitors the incorporation of Texas Red DHPE into the liquid- disordered phase of the lipid membrane. The green channel monitors the binding of Alexa 488 labeled His-tagged HSA to the membrane. Images of GUV with folded HSA and unfolded HSA are overlays of the corresponding red channel and green channel images. The yellow indicates regions of overlap between the two channels, interpreted as co-location of the bound protein and liquid disordered phase. Scale bar 50 μm.

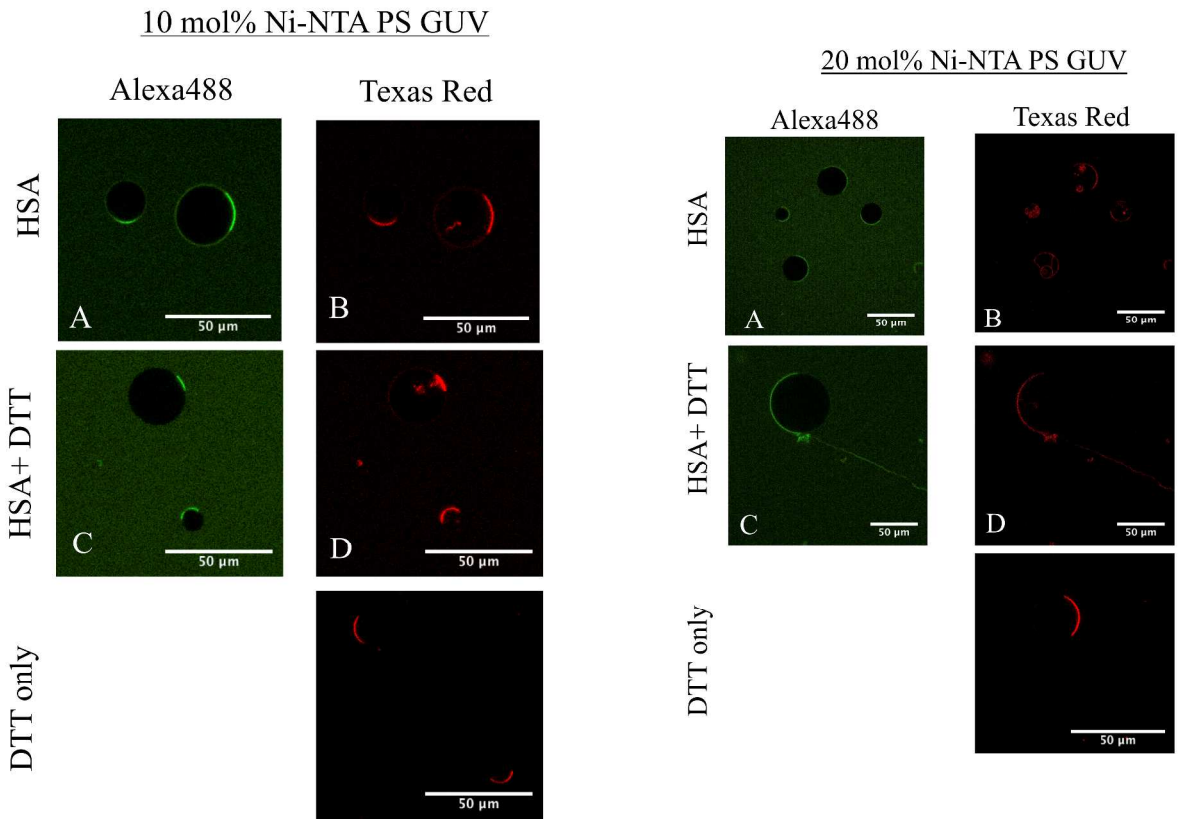

Figure S7. Confocal images of PS GUV doped with 10 mol%, 20 mol%, 30 mol% Ni-NTA-DGS in the presence of DTT, HSA, and unfolded HSA. Green channel is due to Alexa488 labeled His-tagged HSA. Red channel marks liquid disordered phase in GUV labelled with Texas Red DHPE. Scale bar 50 µm long.

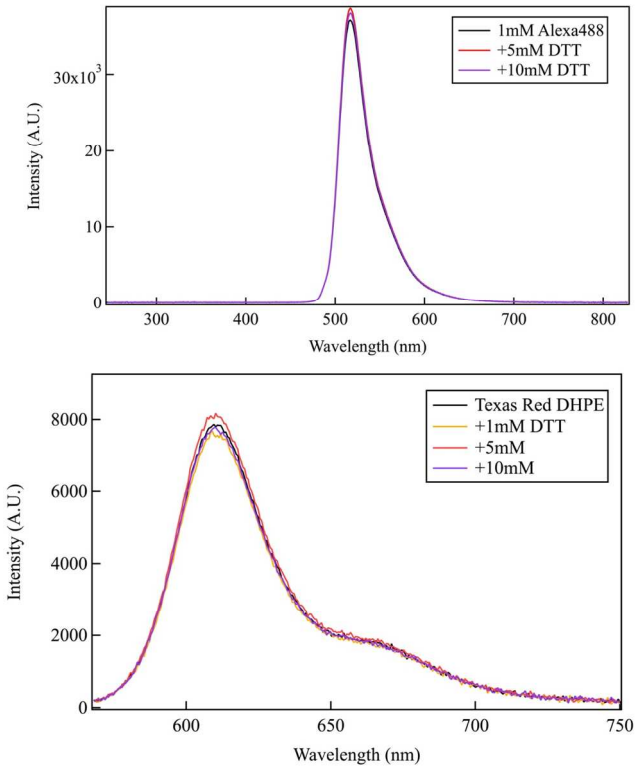

Figure S8. Fluorescence emission spectra of Alexa 488 and Texas Red DHPE in the presence of DTT. Spectra show no shift in emission maxima of Alexa 488 and Texas Red DHPE after incubating with various concentration of DTT. We conclude that DTT does not affect λ_{max} of either dye.

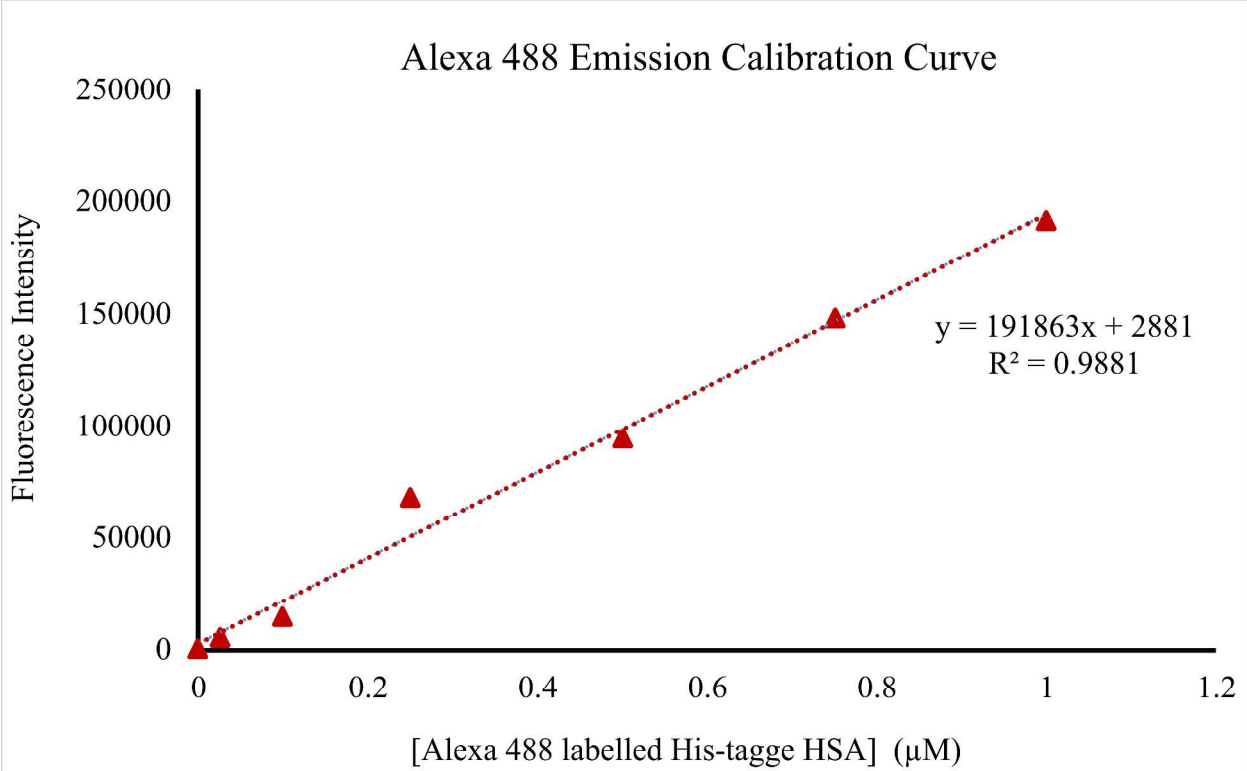

Figure S9. Calibration curve for quantification of His-tagged HSA bound on liposomes. Calibration curve obtained by measuring Alexa 488 fluorescence (λ_{ex}=488nm) of labelled His-tagged HSA without any liposomes at various concentrations (0.05 to 1μM).

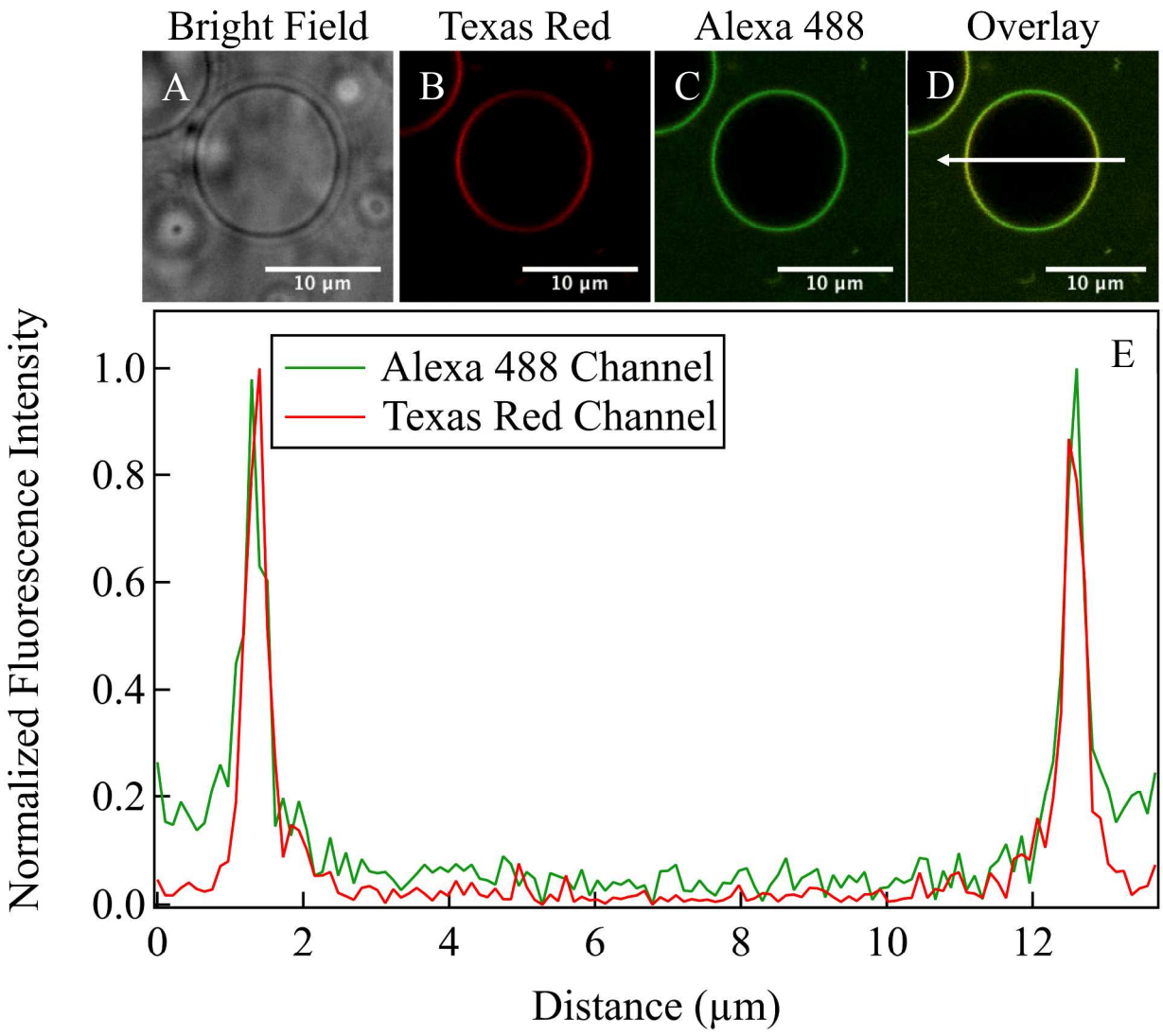

Figure S10. Confocal images of NPSL and corresponding intensity profile A. Confocal imaging with bright field. B. Red channel marks liquid disordered phase in GUV labelled with Texas Red DHPE. C. Green channel marks Alexa488 labeled His-tagged HSA. D. Overlaid image of Texas Red and Alexa 488 channels indicates binding of HSA to liquid-disordered phase. Scale bar 10 µm. E. Fluorescence intensity profile of the overlaid image (indicated by an arrow in the merged GUV image).

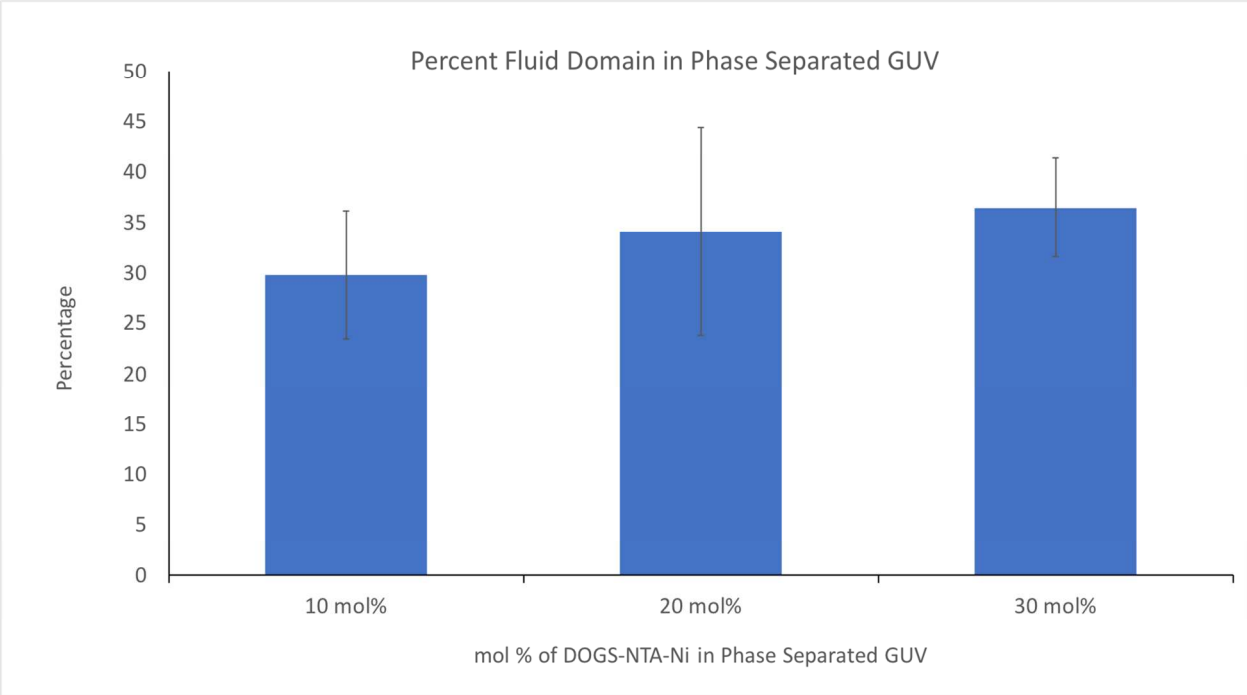

Figure S11. Percentage of surface area occupied by the liquid-disordered domain in phase-separated GUV containing 10 to 30 mol% Ni-NTA-DGS. About 30% of the total vesicle surface area is occupied by the liquid-disordered domain, as quantified from confocal microscopy images.

SUPPLEMENTAL TABLE

Table S1. Percent helicity of folded HSA and reductively unfolded HSA calculated according to equation (2) and MRE at 222nm.

	20 μM HSA	20 μM HSA + 200 mM DTT
% Helicity	55.07 ± 1.66	32.93 ± 1.87

Table S2. Decay Time (μs) obtained from fitting DLS autocorrelation functions to single exponential decay model. Phase- separated liposomes (+10 mol%, 20 mol%, 30 mol% Ni-NTA-DGS in fluid domain) with DTT, folded HSA, and unfolded HSA.

Mol% Ni-NTA-DGS	2mM PS Liposomes (μs)	+ 10mM DTT (μs)	+ 1 μM HSA (μs)	+ 1μM HSA, 10 mM DTT (μs)
10 mol%	176.60 ± 2.17E-05	172.17 ± 3.06E-05	194.51 ± 1.22E-05	197.24 ± 1.80E-05
20 mol%	140.48 ± 3.52E-05	139.68 ± 2.56E-05	160.13 ± 2.00E-05	192.58 ± 2.30E-05
30 mol%	160.40 ± 2.83E-05	160.72 ± 2.52E-05	183.42 ± 2.45E-05	200.97 ± 2.40E-05

Table S3. Decay Time (μs) obtained from fitting DLS autocorrelation functions to single exponential decay model. Non- phase- separated liposomes (+10 mol%, 20 mol%, 30 mol% Ni-NTA-DGS in fluid domain), with DTT, folded HSA, and unfolded HSA.

Mol% Ni-NTA-DGS	2mM NPS Liposomes (μs)	+ 10mM DTT (μs)	+ 1μM HSA (μs)	+ 1μM HSA, 10 mM DTT (μs)
10 mol%	147.03± 2.45E-05	149.21± 2.32E-05	155.52± 2.01E-05	158.46± 2.36E-05
20 mol%	131.77± 2.97E-05	131.52± 3.25E-05	137.60± 2.67E-05	139.39± 2.83E-05
30 mol%	142.14± 1.76E-05	148.84± 2.31E-05	151.58± 2.10E-05	161.55± 2.34E-05

SUPPLEMENTAL MOVIE 1 TITLE:

PS GUV with 20 mol% Ni-NTA and unfolded HSA

SUPPORTING REFERENCES:

[1] Pande, V. S., and Rokhsar, D. S. (1999) *Proc. Natl. Acad. Sci. U.S.A. 96*, 9062-9067.
[2] Angelova, M. I., and Dimitrov, D. S. (1986) *Faraday Discus. Chem. Soc. 81*, 303.
[3] Pattanayak, R., Basak, P., Sen, S., and Bhattacharyya, M. (2017) *Biochem. Biophys. Rep. 10*, 88-93.
[4] Arsov, Z., and Quaroni, L. (2008) *Biochim. Biophys. Acta. 1778*, 880-889.
[5] Hull, M. C., Cambrea, L. R., and Hovis, J. S. (2005) *Anal. Chem. 77*, 6096-6099.
[6] Riddles, P. W., Blakeley, R. L., and Zerner, B. (1979) *Anal. Biochem. 94*, 75-81.
[7] Stachowiak, J. C., Schmid, E. M., Ryan, C. J., Ann, H. S., Sasaki, D. Y., Sherman, M. B., Geissler, P. L., Fletcher, D. A., and Hayden, C. C. (2012) *Nat. Cell. Biol. 14*, 944-949.
[8] Carnahan, N. F., and Starling, K. E. (1969) *J. Chem. Phys. 51*, 635-636.
[9] Lee, J. Y., and Hirose, M. (1992) *J. Biol. Chem. 267*, 14753-14758.
[10] Lauer, S. A., and Nolan, J. P. (2002) *Cytometry 48*, 136-145.
[11] Dorn, I. T., Pawlitschko, K., Pettinger, S. C., and Tampe, R. (1998) *Biol. Chem. 379*, 1151-1159.
[12] Nagle, J. F. (1993) *Biophys. J. 64*, 1476-1481.
[13] Nilsson, T., Lundin, C.R., Nodlund, G., Ädelroth,P., von Ballmoos, C., Brzezinski, P. (2015) *Sci. Rep. 6,* 24113.